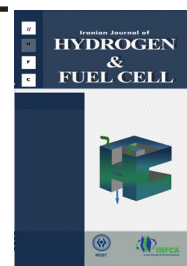


Iranian Journal of Hydrogen &amp; Fuel Cell

**IJHFC**

Journal homepage://ijhfc.irost.ir



## Ni@Pt core-shell nanoparticles as an improved electrocatalyst for ethanol electrooxidation in alkaline media

**Biuck Habibi, Serveh Ghaderi\***

Electroanalytical Chemistry Laboratory, Department of Chemistry, Faculty of Sciences, Azarbaijan Shahid Madani University, Tabriz, Iran

### Article Information

Article History:

Received:

23 October 2015

Received in revised form:

11 December 2015

Accepted:

19 December 2015

### Keywords

Ni@Pt nanoparticles

Core-shell

Electrooxidation

Ethanol

Alkaline media

### Abstract

Core-shell nanostructures are emerging as more important materials than alloy nanostructures and have much more interesting potential applications in various fields. In this work, we demonstrated the fast and facile synthesis of core-shell nanoparticles consisting of a Pt thin layer as the shell and Ni nanoparticles as the cores. The described method herein is suitable for large-scale and low-cost production of core-shell nanoparticles. X-ray diffraction, scanning electron microscopy, transmission electron microscopy and energy dispersive X-ray spectroscopy techniques were used to investigate the physicochemical characterizations. Importantly, the catalytic activity of Ni@Pt core-shell nanoparticles was probed to develop an electrocatalyst in direct ethanol fuel cells (DEFCs). This electrocatalyst was applied to the ethanol oxidation reaction for the first time. Thus, the electrocatalytic activity of the Ni@Pt core-shell nanoparticles towards the ethanol oxidation reaction has been investigated by cyclic voltammetry and chronoamperometry methods in a NaOH solution. The Ni@Pt core-shell nanoparticles show markedly enhanced electrocatalytic activity and stability for ethanol oxidation compared with the Pt nanoparticles catalyst. The results indicate that the  $J_r/J_b$  of Ni@Pt is 1.4 times that of Pt. This high electrocatalytic performance can be attributed to the unique structure of the as-prepared nanoparticles. The attractive performances of Ni@Pt core-shell nanoparticles make them a promising candidate electrocatalyst for ethanol electrooxidation.

## 1. Introduction

In the past few decades, energy demand has been increasing more and more on account of the rapid development of worldwide economy and industry. The global energy crisis and various environmental

problems have worsened in recent years [1, 2]. It is generally accepted that the energy required for our continuously changing world should be attained, as much as possible, through environmentally friendly means [3]. Electrocatalytic energy conversion plays a vital role in the development of sustainable

\*Corresponding Author's E-mail address: Ghaderi@azaruniv.edu, servehghaderi@yahoo.com  
Tel & Fax: +98-41 34327541

technologies for decreasing consumption of fossil fuels and mitigating climate warming [4]. Thus, fuel cell technology has been considered as an effective way to resolve the problem of the exhaustion trend for fossil fuel. Fuel cells directly transform chemical energy to power with high efficiency and potentially zero emission of pollutants. Direct alcohol fuel cells (DAFCs) have attracted increasing interest because of their potential applications in portable electronic devices with high efficiency, low emissions and simple systems [5].

It is known that platinum (Pt) is widely used as a catalyst in DAFCs due to the rapid kinetics of the oxidation and reduction reactions taking place on its surface. But, commercialization of the fuel cells is difficult due to the high-cost and scarcity of Pt. Decreasing the Pt content in fuel cells by synthesizing nanostructures is a suitable route for Pt economy; nanostructures such as core-shell structure where Pt is on the surface of a sacrificial metal core [3]. Core-shell nanoparticles can be regarded as a kind of phase separation of an alloy into a core surrounded by the shell composed of a metal. First, a core-shell construction can be leveraged on the use of a low-cost metal core and a noble metal overlayer to greatly reduce the cost of the electrocatalyst. Second, pure Pt deposited on top of non-Pt substrates can significantly altered surface electrocatalytic activity. This new class of electrocatalysts can be tailored to show an enhanced alcohol oxidation reaction and oxygen reduction reaction kinetics, and at the same time possess improved stability of Pt under typical fuel cell operating conditions [6, 7]. In addition, in recent years there has been considerable interest in the electrochemical oxidation of small organic molecules on nickel-based electrodes because of their potential utility in electroorganic synthesis, development of fuel cells and electrochemical detection in flowing streams [8-10]. Many efforts have been made to prepare the nickel-based core-shell structure electrocatalysts such as Ni@Pt core-shell nanoparticles for the oxygen reduction reaction [11, 12], Ni@Pt core-shell structure electrocatalyst for methanol oxidation [13, 14] and others [15]. It has been shown that the Ni@Pt

core-shell nanoparticles have high activity and excellent stability in comparison with other Pt electrocatalysts.

Here, we reported the synthesis of core-shell nanoparticles (Ni@Pt) with Ni as cores and Pt as shells. The described method herein for producing of the electrocatalyst is facile, suitable for large-scale, and low-cost due to significant lowering of the Pt loading. X-ray diffraction (XRD), scanning electron microscopy (SEM), transmission electron microscopy (TEM) and energy dispersive X-ray spectroscopy (EDX) techniques were used to investigate the physicochemical characterizations of the core-shell nanoparticles. The recent data shows that direct ethanol fuel cells are attractive alternatives for proton exchange membrane fuel cells (PEMFCs) applications. The general electrochemical behavior towards ethanol oxidation on core-shell nanoparticles has been investigated by cyclic voltammetry (CV) and chronoamperometry (CA) methods in a NaOH solution. In this study, we applied Ni@Pt to catalyze ethanol oxidation for the first time and the electrochemical measurements showed that the Ni@Pt catalyst has superior catalytic activity and stability for ethanol electrooxidation compared to Pt nanoparticles. This behavior is due to the modification of the structure and electronic states, such as atomic arrangements and chemical potentials of the interfacial region. This study provides new insights for further developing and designing efficient catalyst materials for DEFC applications.

---

## 2. Experimental

### 2.1. Chemical materials and instrumentation

$\text{H}_2\text{PtCl}_6 \cdot 6\text{H}_2\text{O}$ ,  $\text{NiCl}_2 \cdot 6\text{H}_2\text{O}$ ,  $\text{NaBH}_4$ , ethanol, methanol, HCl, high purity graphite powder and NaOH were obtained from Merck. All these substances were pure and required without further purification. Methyltrimethoxy silane (MTMOS) was obtained from Fluka. All solutions were freshly prepared with distilled water. All electrochemical experiments

were performed in a conventional three-electrode electrochemical cell at room temperature using an AUTOLAB PGSTAT-100 (potentiostat/galvanostat) equipped with a USB electrochemical interface and controlled by GEPS software. A carbon-ceramic electrode (CCE) supported by a catalyst layer (Pt and Ni@Pt nanoparticles) was used as the working electrode. A saturated calomel electrode (SCE) and a platinum wire were used as the reference and the counter electrode, respectively. The surface morphology of the electrocatalyst nanoparticles was characterized by SEM using a LEO1430 vp (Carl Zeiss, Germany) instrument equipped with an energy dispersion X-ray spectroscopy device. The TEM measurement was made on a Carl Zeiss 906 E (Cottingen, Germany) microscope with a 10 kV accelerating voltage and grid size 200 meshes. The powder XRD measurements of the samples were recorded on a Bruker AXS model D<sub>8</sub> Advance (Karlsruhe, Germany) instrument with a Cu-K<sub>α</sub> radiation source (1.54 Å) at 40 kV and 35 mA. The 2θ angular regions between 20° and 80° were explored at a scan rate of 5° min<sup>-1</sup>.

## 2.2. Synthesis of the Ni @Pt nanoparticles

The Ni@Pt nanoparticles were prepared using NiCl<sub>2</sub>·6H<sub>2</sub>O and H<sub>2</sub>PtCl<sub>6</sub>·6H<sub>2</sub>O as metallic precursors and NaBH<sub>4</sub> as reducing agent. To obtain the Ni cores, the metallic salt solution [NiCl<sub>2</sub>·6H<sub>2</sub>O, 0.02 M] was added dropwise into the solution containing the reducing agent [NaBH<sub>4</sub>, 0.01 M] at room temperature and magnetically stirred. The obtained product was washed and separated by centrifugation at 3000 rpm. To obtain the Ni@Pt nanoparticles, the cores were suspended in a fresh reducing solution of NaBH<sub>4</sub> (0.01 M); then, a solution of H<sub>2</sub>PtCl<sub>6</sub>·6H<sub>2</sub>O (0.02 M) was slowly added under magnetically stirring and the mixture was stirred for 30 min at 25°C [16]. During this period, the color of the mixture gradually turned from light red to dark black indicating Ni@Pt nanoparticles had been formed. Finally, the obtained product was separated by centrifugation at 3000 rpm, washed and dried.

## 2.3. Preparation of the electrocatalyst

The electrocatalyst was prepared in a two-step process. The first step, the sol-gel derived carbon-ceramic electrode (CCE) was constructed the same as in our previous works [17, 9]. Firstly, a portion of 0.9 mL MTMOS was mixed with 0.6 mL methanol and 0.6 mL of 0.5 M HCl as the catalyst. The mixture was magnetically stirred until a homogeneous solution resulted. Next, 0.3 g of graphite powder was added and the mixture was shaken for several minutes. Subsequently, the homogenized mixture was tightly packed into a Teflon tube (with 3.9 mm inner diameter and 10 mm length) and dried for at least 24 h at room temperature. A copper wire was inserted through the other end to set up an electric contact. The obtained CCE was polished with 1500 emery paper and was rinsed with double distilled water. In the second step, 20 mg of Ni@Pt nanoparticles were ultrasonically suspended in a 5 mL solution containing 50 μL Nafion (5% wt) in double distilled water for 30 min to obtain a uniform ink. Then, 5 μL of the prepared Ni@Pt nanoparticles ink was transferred onto the top of the freshly polished CCE surface and was allowed to dry at room temperature. For comparison, the monometallic electrocatalyst, Pt (Pt on the CCE), was also prepared using the same approach without Ni cores.

## 3. Results and discussion

### 3.1. Physicochemical characterization of Ni@Pt nanoparticles

The formation, crystallites and lattice parameters of the Ni@Pt nanoparticles were characterized using the XRD technique. The XRD patterns of Pt and Ni@Pt nanoparticles are shown in Figure 1. The diffractogram of the Pt nanoparticles (Figure 1 (A)) has four diffraction peaks centered at Bragg angles of about 39.96°, 46.76°, 67.96° and 81.36° that can be assigned to the (111), (200), (220) and (311) facets of the Pt face centered cubic (fcc) lattice structure [18]. With the presence of Ni in the face centered cubic

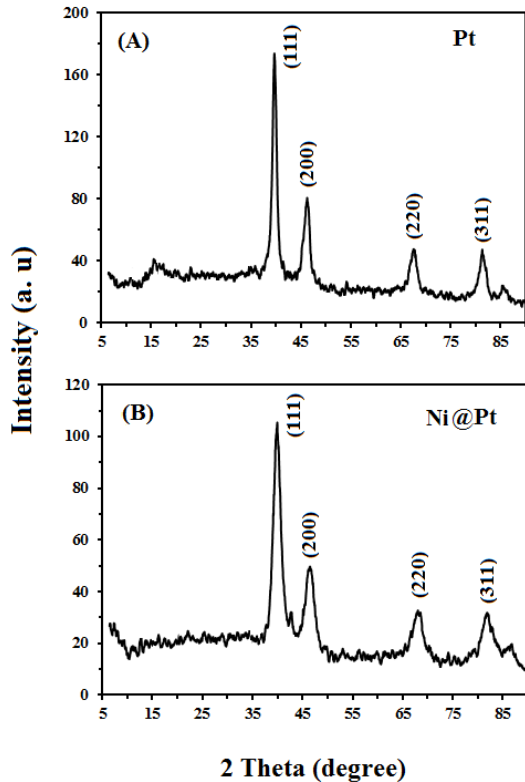


Fig. 1. XRD patterns of (A) Pt nanoparticles and (B) the Ni@Pt core-shell nanoparticles.

(fcc) structure of Pt, the Pt reflections are slightly shifted (positive shift) to higher values of  $2\theta$  (Figure 1 (B)), which show a contraction of the lattice and the formation of Ni@Pt core-shell nanoparticles [19]. Based on the XRD results (absence of Ni diffraction peaks and slightly positive shift of the Pt diffraction peaks), it can be confirmed that the Ni@Pt core-shell nanoparticles are composed of a Ni core with Pt shell cladding.

The surface morphology and chemical structural characterization of Ni@Pt nanoparticles were further investigated by SEM and the corresponding results are shown in Figure 2. As can be seen, the Ni@Pt nanoparticles exhibit a very uniform distribution and homogeneous range in size with a globular structure. In order to specify the chemical composition of the Ni@Pt nanoparticles an EDX analysis was used (inset of Figure 2). The presence of Pt (main peak with high percentage) and the negligible presence of a Ni on the other hand, TEM investigation shows the formation of the core-shell nanoparticles (Figure 3).

element confirmed that the Ni cores were completely coated by the Pt shells.

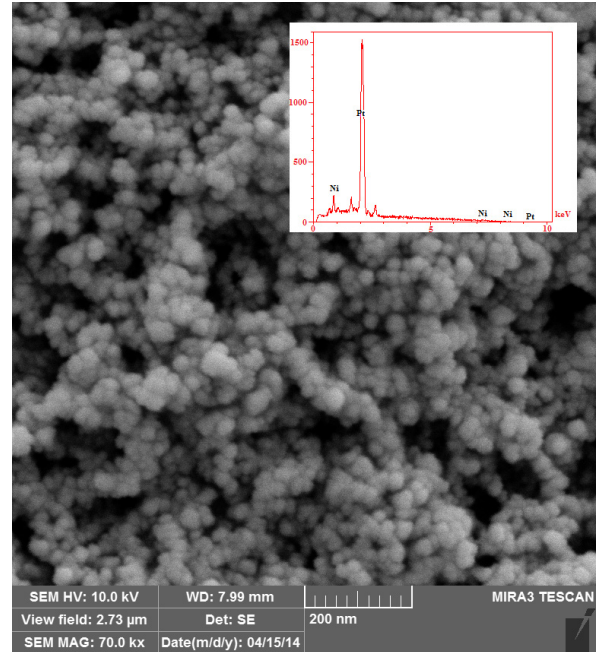


Fig. 2. SEM image of Ni@Pt core-shell nanoparticles (The inset shows EDX spectrum of Ni@Pt nanoparticles).

The Ni@Pt nanoparticles size distribution was calculated based on random counting of particles from TEM image analysis. The histogram for particles size

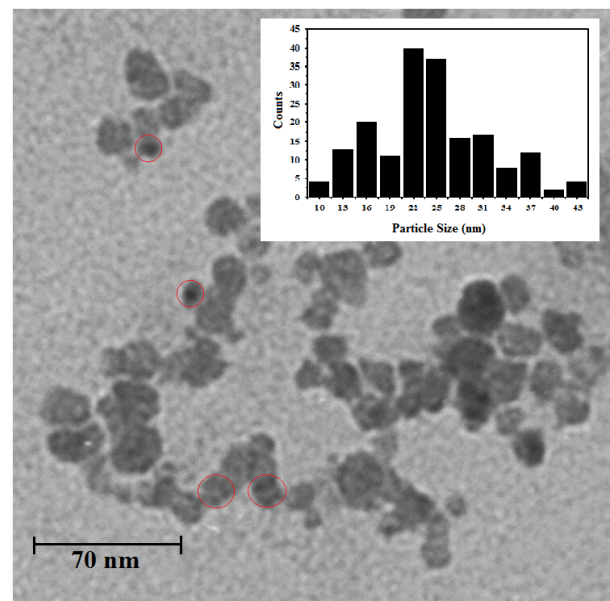


Fig. 3. TEM image of Ni@Pt core-shell nanoparticles (The inset shows particle size distribution from several different regions).

distribution (inset of Figure 3) includes analysis of several different regions of the nanoparticles. The as-prepared Ni@Pt nanoparticles have spherical shapes with an average diameter of approximately 20-30 nm which agreed fairly well with the SEM images.

### 3.2. Electrochemical characterization of Ni@Pt

Cyclic voltammogram of Ni@Pt nanoparticles in 0.5 M NaOH solution at a scan rate of 50 mV s<sup>-1</sup> is shown in Figure 4. Also, the cyclic voltammogram of the Pt nanoparticles for comparison is shown in the same figure. As seen, there exist two pairs of distinct peaks in the hydrogen region between -1.1 and 0.4 V. A broad oxidation peak in the potential greater than -0.4 V on the positive-going scan has been noticed, which can be attributed to transformation of the Pt metal present in the surface electrocatalyst into Pt (II) oxide (PtO). The corresponding peak between -0.7 and -0.2 V is ascribed to the reduction of Pt (II) oxide into elemental Pt.

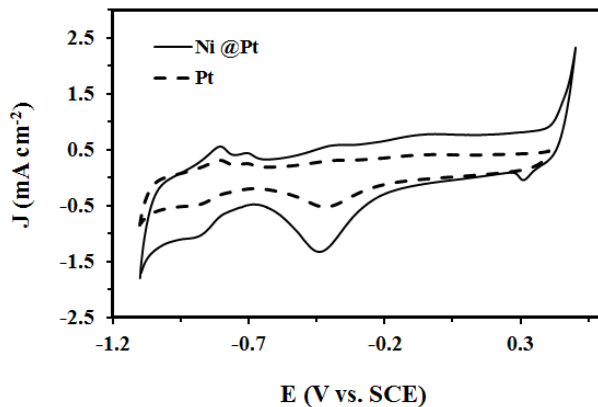


Fig. 4. Cyclic voltammograms of Ni@Pt and Pt catalysts in 0.5 M NaOH electrolyte at room temperature and at scan rate of 50 mV s<sup>-1</sup>.

The electrochemical active surface area (EASA) is an important factor in the characterization of an electrocatalyst. The EASA of the Ni@Pt electrocatalyst was measured by determining of the coulombic charge associated to the hydrogen adsorption/desorption. The anodic and cathodic peaks

at the potential range from -1.1 to -0.7 V are due to the adsorption/desorption of hydrogen. The EASA was calculated from the following equation [19]:

$$EASA(m^2 g^{-1} Pt) = Q_H / [Q_{ref} \times Pt \text{ loading}]$$

In which  $Q_H$  indicates the coulombic integrated charge associated with the hydrogen adsorption region (mC),  $Q_{ref}$  has a corresponding value of 0.21 mC cm<sup>-2</sup>, which is the charge for a monolayer adsorption of hydrogen on the surface of Pt. The EASA value for Ni@Pt from the hydrogen adsorption/desorption peaks was obtained as 4.2 cm<sup>2</sup> g<sup>-1</sup> as compared to 1.9 cm<sup>2</sup> g<sup>-1</sup> for Pt. The EASA of the Ni@Pt is 2.2 times higher than that of the Pt, confirming that the core-shell electrocatalyst could improve the use ratio of the Pt metal [5, 20].

To evaluate the electrocatalytic activity of the Ni@Pt catalyst, cyclic voltammetry of ethanol electrooxidation was recorded in a 0.5 M NaOH + 0.5 M ethanol solution at room temperature. Also, The Pt catalyst was tested under the same conditions for comparison. The obtained cyclic voltammetry profiles on the present electrocatalysts at a scan rate of 50 mV s<sup>-1</sup> are shown in Figure 5. The electrooxidation

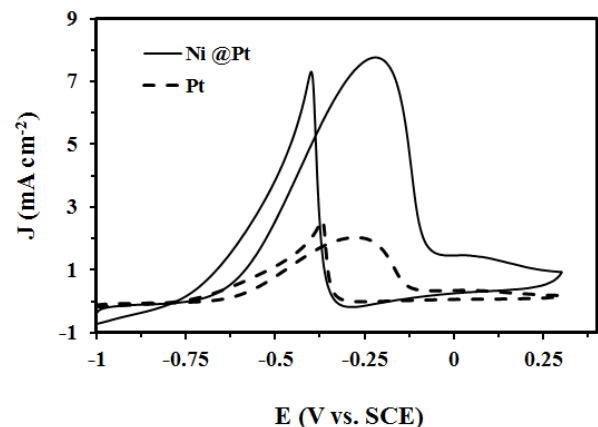


Fig. 5. Cyclic voltammograms of the Ni@Pt and Pt catalysts modified electrodes in 0.5 M ethanol + 0.5 M NaOH at scan rate of 50 mV s<sup>-1</sup>.

of ethanol shows only one main peak in both the forward and reverse scan directions and the oxidation current densities of ethanol on the Ni@Pt

are significantly higher than that of the Pt. The large anodic peak in the reverse scan is attributed to the removal of the incompletely oxidized carbonaceous species formed in the forward scan [21].

The results of the cyclic voltammogram curves indicate that the peak potential of the ethanol electrooxidation in the forward scan on the Ni@Pt catalyst is almost the same as that of the Pt catalyst, but the peak current density of the Ni@Pt catalyst for the ethanol electrooxidation in the forward scan is 4 times higher than that of the Pt catalyst. Also, the onset potential of the Ni@Pt catalyst (-0.75 V) is 100 mV lower than that of the Pt catalyst (-0.65 V). It was concluded that the improved anodic peak current density, enhanced electrode kinetics, enhanced electrocatalytic activity and rare metal utilization on the Ni@Pt catalyst must be due to the induced geometric effect by the formation of core-shell structure, better dispersion of Pt and the higher EASA. This allows a greater number of catalytically active sites to be present on the available surface of the particles as Ni was contained in the underlying core. Furthermore, due to the synergetic effect between Ni and Pt elements, the inter-atomic Pt-Pt distances in the Ni@Pt catalyst might be changed, which can result in more facile fuel adsorption and oxidation due to the modified surface and electronic properties [22, 23]. On the other hand, as reported in the literature [24, 25], the ratio of the forward peak current density to reverse peak current density ( $J_f/J_b$ ) is generally used to characterize of tolerance to CO-like oxidative intermediates generated during the

oxidation reaction of alcohol. A high  $J_f/J_b$  indicates more effective removal of the poisoning species from the electrocatalyst surface. In this work, the  $J_f/J_b$  value for Ni@Pt catalyst is 1.1, which is 1.4 times higher than that of the Pt catalyst (0.8), an indication of the Ni@Pt catalyst's greater poisoning tolerance to CO-like intermediates, due to its unique core-shell structure and enhanced Pt utilization. The high electrocatalytic activity and good tolerance to  $\text{CO}_{\text{ads}}$  on the Ni@Pt catalyst is consistent with the literature [5, 26, 27].

For a fair assessment of the results in various literature, we present a comprehensive comparative (Table 1) where the electroactivity of the Ni@Pt catalyst is compared with the electroactivity of other catalysts in relevant literature. Table 1 confirms that Ni@Pt exhibits better catalytic performance than several literature reports to date.

### 3.3. Effect of scan rate

For obtaining information about the transport characteristics of the ethanol oxidation, the influence of the scan rate ( $v$ ) in the oxidation of ethanol on the Ni@Pt electrocatalyst was investigated (Figure 6). Variation of the peak current density as a function of scan rate was given in Figure 7 (A). It can be understood from this observation that the forward oxidation peak current density positively shifts as the scan rate increases. The anodic peak current densities are linearly proportional to the square root of the scan

**Table 1: Comparison of different modified electrodes for ethanol oxidation reaction.**

Electrocatalyst	Specific conditions	J (mA cm <sup>-2</sup> )	Ref.
Ni@Pt	0.5 M NaOH+ 0.5 M EtOH, 50 mV s <sup>-1</sup>	7.76	This work
PdSnAg	1.0 M KOH + 1.0 M EtOH, 50 mV s <sup>-1</sup>	3.37	[2]
PdSnNi	1.0 M KOH + 1.0 M EtOH, 50 mV s <sup>-1</sup>	2.23	[2]
PdNi	1.0 M KOH + 1.0 M EtOH, 50 mV s <sup>-1</sup>	0.69	[4]
PdCo	1.0 M KOH + 1.0 M EtOH, 50 mV s <sup>-1</sup>	8.76	[4]
Ru@PtPd	1.0 M KOH + 1.0 M EtOH, 50 mV s <sup>-1</sup>	3.6	[26]
FeCo@Fe@Pd	0.5 M KOH + 0.5 M EtOH, 50 mV s <sup>-1</sup>	3.93	[28]
PdNiCeO	1.0 M KOH + 1.0 M EtOH, 50 mV s <sup>-1</sup>	5.3	[29]
Te@Au	1.0 M KOH + 1.0 M EtOH, 50 mV s <sup>-1</sup>	12	[30]

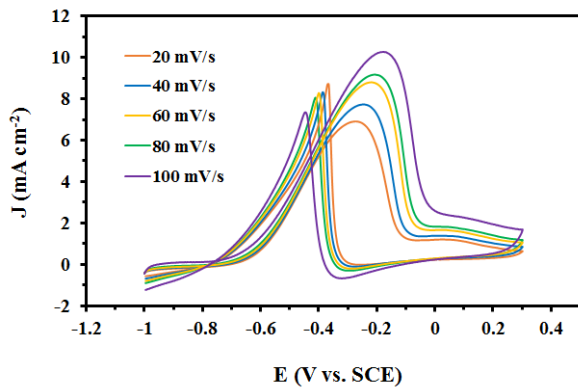


Fig. 6. Cyclic voltammograms of Ni@Pt catalyst in 0.5 M ethanol + 0.5 M NaOH at different scan rates (20, 40, 60, 80 and 100  $\text{mV s}^{-1}$ ).

rate, which suggests that the electrocatalytic oxidation of ethanol on the Ni@Pt is a diffusion controlled process [31]. Potential of forward scan peaks increases with the increase of scan rate and there is a linear relationship between  $E_p$  and  $\ln(v)$  (Figure 7 (B)). It shows that the oxidation of ethanol is an irreversible electrode process [32].

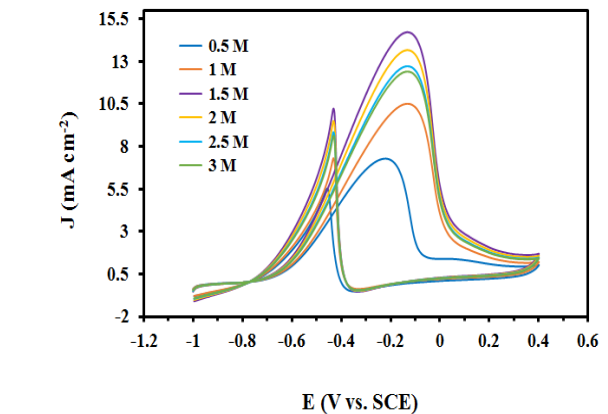
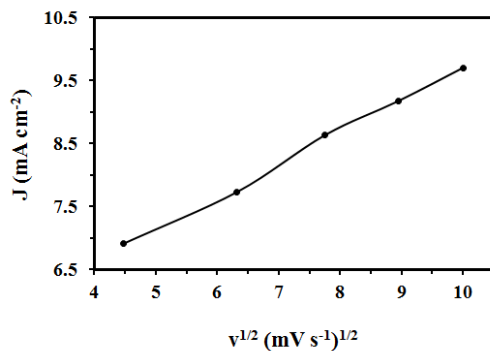


Fig. 8. Cyclic voltammograms of Ni@Pt catalyst in various fuel concentrations (0.5, 1, 1.5, 2, 2.5 and 3 M).

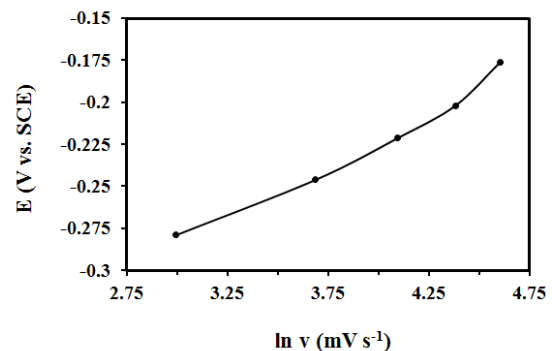


Fig. 7. Plot of the peak current density versus the square root of scan rate (A) and plot of E (V vs. SCE) versus the  $\ln v$  ( $\text{mV s}^{-1}$ ) (B).

### 3.4. The effect of ethanol concentration

In order to assess the capacity of the Ni@Pt against ethanol oxidation, the effect of different concentrations on the anodic peak current density was investigated (Figure 8). It can clearly be seen that by increasing the ethanol concentration, the peak current density increases and drops afterward in concentrations higher than 1.5 M (Figure 9). This effect might be due to the

saturation of the Pt active sites by ethanol molecules and also contamination of the catalyst surface which mainly arises from the  $\text{CO}_{\text{ads}}$  during the oxidation reaction. In accordance with this result, the optimum ethanol concentration to achieve a higher peak current density may be considered as about 1.5 M.

### 3.5. Chronoamperometric study

Chronoamperometric experiments were carried out for further evaluation of the catalytic activity and stability of the catalyst under a period of time of continuous operation. Chronoamperometric experiments were widely applied to explore the catalytic stability and reactive mechanism [33, 34]. Figure 10 shows the chronoamperometry curves of 0.5 M NaOH + 0.5 M

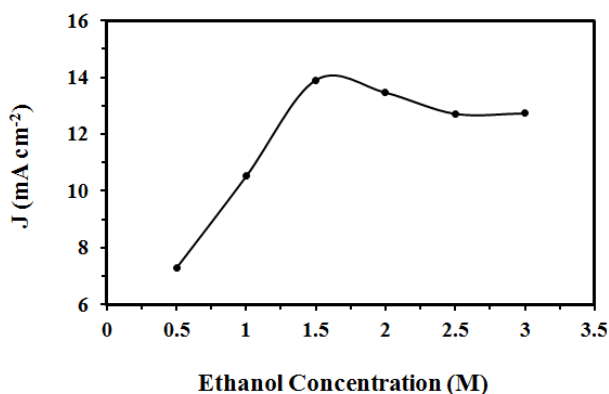


Fig. 9. Plot of the peak current density versus ethanol concentration at scan rate of  $50 \text{ mV s}^{-1}$ .

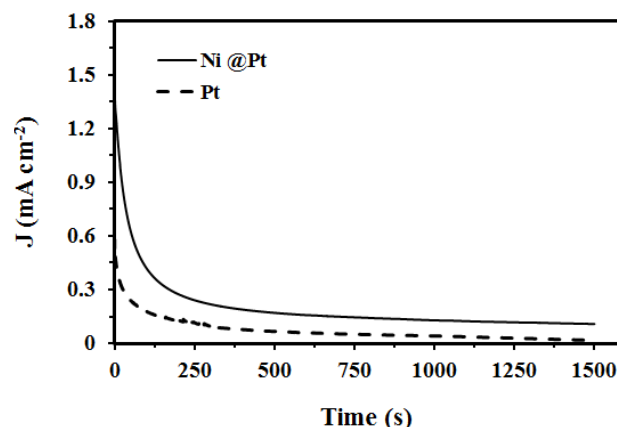


Fig. 10. Chronoamperometry curves for Ni@Pt and Pt recorded in  $0.5 \text{ M ethanol} + 0.5 \text{ M NaOH}$  solution at  $-0.2 \text{ V}$ .

ethanol solution on the Ni@Pt and Pt electrode at  $-0.2 \text{ V}$  for  $1500 \text{ s}$ . An initial fast current decay in chronoamperometry curves was possibly due to the electrocatalyst poisoning by the chemisorbed CO-like intermediate species and the formation of some Pt (and/or Ni) oxides/hydroxides during the continuous ethanol electrooxidation process [35]. Intermediate species and Pt (and/or Ni) oxides/hydroxides tend to accumulate on the accessible catalytic sites. A further gradual decay of current density with time implies that the catalyst has good anti-poisoning ability [36]. During the whole procedure, the Ni@Pt catalyst exhibited a higher current density and lower decay rate of current density than Pt. The results are in good agreement with voltammetric studies and indicate that the presence of reactive  $\text{Ni(OH)}_{\text{ad}}$  species in alkaline solution improves the tolerance of Pt nanoparticles against the poisoning species such as CO and CO-like intermediates, thus improving the catalytic activity and the stability of Pt nanoparticles.

#### 4. Conclusion

In summary, we have reported a rapid and easy method to prepare Ni@Pt core-shell nanoparticles. The synthesis process is simple and without the use of expensive chemicals. The prepared electrocatalyst is extensively characterized by XRD, SEM, EDX and TEM techniques. The catalytic activity catalyst

toward ethanol oxidation was evaluated by cyclic voltammetry and chronoamperometry amusements. Results showed that the catalyst has considerably enhanced activity toward ethanol electro-oxidation compared with a Pt catalyst. These behaviors are attributed to an electronic effect of the inner Ni or the increase in the d-orbital vacancy of Pt in the Ni@Pt core-shell catalyst. These results implied that a Ni@Pt core-shell electrocatalyst is very promising for portable applications in the DEFC field. These nanostructures have obvious structural advantages in phrases of unique catalytic properties, easy and clean processing and saving expensive metals which suggest their great potential for use in fuel cell technologies. We believe that the concept of core-shell structures as well as the fabrication technique can be used not only for fuel cell catalysts but also potentially extended to other fields such as electro-chemical sensing and photo-electrochemistry.

#### 5. References

- [1] Lu X., Luo F., Song H., Liao Sh., Li H., "Pulse electrodeposition to prepare core-shell structured AuPt@Pd/C catalyst for formic acid fuel cell application", *J. Power Sources*, 2014, 246: 659.
- [2] Zhu F., Wang M., He Y., Guanshui M., Zhang Zh., Wang X., "A comparative study of elemental additives



- (Ni, Co and Ag) on electrocatalytic activity improvement of PdSn-based catalysts for ethanol and formic acid electro-oxidation”, *Electrochim Acta*, 2014, 148: 291.
- [3] Caballero-Manrique G., Velázquez-Palenzuela A., Brillas E., Centellas F., Garrido J. A., Rodríguez R. M., Cabot P. L., “Electrochemical synthesis and characterization of carbon-supported Pt and Pt-Ru nanoparticles with Cu cores for CO and methanol oxidation in polymer electrolyte fuel cells”, *Int. J. Hydrogen Energy*, 2014, 39: 12859.
- [4] Wang X., Ma G., Zhu F., Lin N., Tang B., Zhang Zh., “Preparation and characterization of micro-arc-induced Pd/TM (TM =Ni, Co and Ti) catalysts and comparison of their electrocatalytic activities toward ethanol oxidation”, *Electrochim Acta*, 2013, 114: 500.
- [5] Zhang M., Yan Z., Xie J., “Core/shell Ni@Pd nanoparticles supported on MWCNTs at improved electrocatalytic performance for alcohol oxidation in alkaline media”, *Electrochim Acta*, 2012, 77: 237.
- [6] Wang H., Wang R., Li H., Wang Q., Kang J., Lei Z., “Facile synthesis of carbon-supported pseudo-core@shell PdCu@Pt nanoparticles for direct methanol fuel cells”, *Int. J. Hydrogen Energy*, 2011, 36: 839.
- [7] Chaudhuri R. Gh., Paria S., “Core/Shell Nanoparticles: Classes, Properties, Synthesis Mechanisms, Characterization, and Applications”, *Chem. Rev*, 2012, 112: 2373.
- [8] Ciszewski A., Milczarek G., “Kinetics of electrocatalytic oxidation of formaldehyde on a nickel porphyrin-based glassy carbon electrode”, *J. Electroanal Chem*, 1999, 469: 18.
- [9] Habibi B., Delnavaz N., “Carbon-ceramic supported bimetallic Pt-Ni nanoparticles as an electrocatalyst for oxidation of formic acid”, *Int. J. Hydrogen Energy*, 2011, 36: 9581.
- [10] Chen Y., Yang F., Dai Y., Wang W., Chen Sh., “Ni@Pt Core-Shell Nanoparticles: Synthesis, Structural and Electrochemical Properties”, *J. Phys. Chem. C*, 2008, 112: 1645.
- [11] Wang G., Wu H., Wexler D., Liu H., Savadogo O., “Ni@Pt core-shell nanoparticles with enhanced catalytic activity for oxygen reduction reaction” *J. Alloys Compd*, 2010, 503: L1.
- [12] Cantane D.A., Oliveira F. E. R., Santos S. F., Lima F. H. B., “Synthesis of Pt-based hollow nanoparticles using carbon-supported Co@Pt and Ni@Pt core-shell structures as templates: Electrocatalytic activity for the oxygen reduction reaction”, *Appl. Catal. B: Environmental*, 2013, 136: 351.
- [13] Ding L-X., Li G-R., Wang Z-L., Liu Zh-Q., Liu H., Tong Y-X., “Porous Ni@Pt Core-Shell Nanotube Array Electrocatalyst with High Activity and Stability for Methanol Oxidation”, *Chem. Eur. J*, 2012, 18: 8386.
- [14] Fu X-Zh., Liang Y., Chen Sh-P., Lin J-D., Liao D-W., “Pt-rich shell coated Ni nanoparticles as catalysts for methanol electro-oxidation in alkaline media”, *Catal. Commun*, 2009, 10: 1893.
- [15] Bhlapibul S., Pruksathorn K., Piumsomboon P., “The effect of the stabilizer on the properties of a synthetic Nicore-Ptshell catalyst for PEM fuel cells”, *Renewable Energy*, 2012, 41: 262.
- [16] Sañchez-Padilla N. M., Montemayor S. M., Torres L. A., Rodríguez Varela F. J., “Fast synthesis and electrocatalytic activity of M@Pt (M [Ru, Fe<sub>3</sub>O<sub>4</sub>, Pd]) core-shell nanostructures for the oxidation of ethanol and methanol”, *Int. J. Hydrogen Energy*, 2013, 38: 12681.
- [17] Habibi B., Dadashpour E., “Carbon-ceramic supported bimetallic Pt-Ni nanoparticles as an electrocatalyst for electrooxidation of methanol and ethanol in acidic media”, *Int. J. Hydrogen Energy*, 2013, 38: 5425.
- [18] Li Z., He Ch., Caib M., Kang Sh., Shen P. K., “A strategy for easy synthesis of carbon supported Co@Pt core-shell configuration as highly active catalyst for oxygen

- reduction reaction”, *Int. J. Hydrogen Energy*, 2012, 37: 14152.
- [19] Ruiz Camacho B., Moraisa C., Valenzuela M. A., Alonso-Vantea N., “Enhancing oxygen reduction reaction activity and stability of platinum via oxide-carbon composites”, *Catal Today*, 2013, 202: 36.
- [20] Xu W., Zhua Sh., Li Zh., Cui Zh., Yang X., “Synthesis and catalytic properties of Pd nanoparticles loaded nanoporous TiO<sub>2</sub> material”, *Electrochim Acta*, 2013, 114: 35.
- [21] Li Sh. Sh., Hu Y. Y., Feng J. J., Lv Z. Y., Chen J. R., Wang A. J., “Rapid room-temperature synthesis of Pd nanodendrites on reduced graphene oxide for catalytic oxidation of ethylene glycol and glycerol”, *Int. J. Hydrogen Energy*, 2014, 39: 3730.
- [22] Lin R., Cao Ch., Zhao T., Huang Zh., Li B., Wieckowski A., Ma J., “Synthesis and application of core-shell Co@Pt/C electrocatalysts for proton exchange membrane fuel cells”, *J. Power Sources*, 2013, 223: 190.
- [23] Santiago E. I., Varanda L. C., Villullas M. J., “Carbon-supported Pt-Co catalyst prepared by a modified polyol process as cathodes for PEM fuel cells”, *J. Phys. Chem. C*, 2007, 111: 3146.
- [24] Divya P., Ramaprabhu S., “Platinum nanoparticles supported on a bi-metal oxide grown carbon nanostructure as an ethanol electro-oxidation electrocatalyst”, *J. Mater. Chem. A*, 2013, 1: 13605.
- [25] Hasan M., Newcomb S. B., Razeeb K. M., “Porous Core/Shell Ni@NiO/Pt Hybrid Nanowire Arrays as a High Efficient Electrocatalyst for Alkaline Direct Ethanol Fuel Cells”. *J. Electrochem. Soc.* 2012, 159: F203.
- [26] Gao H., Liao Sh., Liang Zh., Liang H., Luo F., “Anodic oxidation of ethanol on core-shell structured Ru@PtPd/C catalyst in alkaline media”. *J. Power Sources*, 2011, 196:6138.
- [27] Zhang Z. Y., Xin L., Sun K., Li W. Z., “Pd–Ni electrocatalysts for efficient ethanol oxidation reaction in alkaline electrolyte”, *Int. J. Hydrogen Energy*, 2011, 36: 12686.
- [28] Fashedemi O. O., Ozoemena K. I., “Comparative electrocatalytic oxidation of ethanol, ethylene glycol and glycerol in alkaline medium at Pd-decorated FeCo@Fe/C core-shellnanocatalysts”, *Electrochim Acta*, 2014, 128: 279.
- [29] Wei Y.-C., Liu C.-W., Kang W.-D., Lai C.-M., Tsai L.-D., Wang K.-W., “Electro-catalytic activity enhancement of Pd–Ni electrocatalysts for the ethanol electro-oxidation in alkaline medium: The promotional effect of CeO<sub>2</sub> addition”, *J. Electroanal. Chem*, 2011, 660: 64.
- [30] Jin H., Wang D., Zhao Y., Zhou H., Wang Sh., Wang J., “Fabrication of Te@Au core-shell hybrids for efficient ethanol oxidation”, *J. Power Sources*, 2012, 215: 227.
- [31] Yang S., Zhang X., Mi H., Ye X., “Pd nanoparticles supported on functionalized multi-wall carbon nanotubes (MWCNTs) and electrooxidation for formic acid”, *J. Power Sources*, 2008, 175: 26.
- [32] Wang J. Y., Kang Y. Y., Yang H., Cai W. B., “Boron-doped palladium nanoparticles on carbon black as a superior catalyst for formic acid electro-oxidation”, *J. Phys. Chem C*, 2009, 113: 8366.
- [33] Abbaspour A., Norouz-Sarvestani F., “High electrocatalytic effect of Au-Pd alloy nanoparticles electrodeposited on microwave assisted sol-gel-derived carbon ceramic electrode for hydrogen evolution reaction”, *Int. J. Hydrogen Energy*, 2013, 38: 1883.
- [34] Wang X. M., Xia Y. Y., “The influence of the crystal structure of TiO<sub>2</sub> support material on Pd catalysts for formic acid electrooxidation”, *Electrochim Acta*, 2010, 55: 851.
- [35] Zang J., Dong L., Jia Y., Pan H., Gao Zh., Wang Y., “Core-shell structured SiC@C supported platinum electrocatalysts for direct methanol fuel cells”, *Appl Catal*

B Environ, 2014, 11: 166.

[36] Zhang X., Zhu H., Guo Zh., Wei Y., Wang F., “Design and preparation of CNT@SnO<sub>2</sub> core-shell composites with thin shell and its application for ethanol oxidation”, Int. J. Hydrogen Energy, 2010, 35: 8841.